

Coupled free-carrier and exciton relaxation in optically excited semiconductors

Original

Coupled free-carrier and exciton relaxation in optically excited semiconductors / Selbmann, P. E.; Gulia, M.; Rossi, Fausto; Molinari, E.; Lugli, P.. - In: PHYSICAL REVIEW. B, CONDENSED MATTER. - ISSN 0163-1829. - 54:7(1996), pp. 4660-4673. [10.1103/PhysRevB.54.4660]

Availability:

This version is available at: 11583/2498573 since:

Publisher:

APS

Published

DOI:10.1103/PhysRevB.54.4660

Terms of use:

This article is made available under terms and conditions as specified in the corresponding bibliographic description in the repository

Publisher copyright

(Article begins on next page)

Coupled free-carrier and exciton relaxation in optically excited semiconductors

Peter E. Selbmann, Mario Gulia, Fausto Rossi, and Elisa Molinari

*Istituto Nazionale di Fisica della Materia and Dipartimento di Fisica, Università degli Studi di Modena,
Via G. Campi 213A, I-41100 Modena, Italy*

Paolo Lugli

*Istituto Nazionale di Fisica della Materia and Dipartimento di Ingegneria Elettronica, Università di Roma "Tor Vergata,"
Via della Ricerca Scientifica, I-00133 Roma, Italy*

(Received 1 March 1996)

The energy relaxation of coupled free-carrier and exciton populations in semiconductors after low-density ultrafast optical excitation is studied through a kinetic approach. The set of semiclassical Boltzmann equations, usually written for electron and hole populations only, is complemented by an additional equation for the exciton distribution. The equations are coupled by reaction terms describing phonon-mediated exciton binding and dissociation. All the other relevant scattering mechanisms, such as carrier-carrier, carrier-phonon, and exciton-phonon interactions, are also included. The resulting system of rate equations in reciprocal space is solved by an extended ensemble Monte Carlo method. As a first application, we show results for the dynamics of bulk GaAs in the range from 1 to ~ 200 ps after photoexcitation. The build-up of an exciton population and its sensitivity to the excitation conditions are discussed in detail. As a consequence of the pronounced energy dependence of the LO-phonon-assisted transition probabilities between free-pair states and excitons, it is found that the efficiency of the exciton-formation process and the temporal evolution of the resulting population are sensitive to the excitation energy. We discuss the effects on luminescence experiments. [S0163-1829(96)06831-2]

I. INTRODUCTION

Ultrafast optical excitation of semiconductors at energies well above the fundamental band gap is followed by a rapid relaxation of the initial nonequilibrium state of the system. The recent progress in the generation of extremely short laser pulses¹ and the detection of optical signals on the same time scale has opened the possibility to probe directly these relaxation processes which typically take place in a range of femtoseconds to picoseconds.^{2,3}

A variety of interaction mechanisms contributes to the temporal evolution of the generated hot-electron and -hole distributions. Their relative importance is determined by the actual experimental conditions, in particular by the excess energy and the intensity of the exciting laser and by the lattice temperature. Carrier-carrier scattering leads to a broadening of initially sharp structures in the distribution functions and tends to establish a quasiequilibrium condition among the particles within the different bands. Due to screening and phase-space filling, this effect is strongly dependent on the carrier density. Interaction with different phonon modes acts as coupling to a heat bath which can be driven out of equilibrium itself in case of large excess energies and high carrier densities. The resulting hot-phonon effects will slow down the carrier cooling.

Many of these relaxation processes have been successfully described by a semiclassical theory in terms of Boltzmann equations which have been solved numerically using parametrizations of the distribution functions,⁴⁻⁸ direct-integration methods,^{9,10} eigenfunction expansions,¹¹ and Monte Carlo simulations.¹¹⁻¹⁷ The kinetic variables in these theoretical approaches are the single-particle distribution

functions; the interaction between carriers and various quasiparticles is treated in terms of scattering processes only. While some interaction is implicitly included as a mean field in the definition of the band structure and some may be included effectively in the dielectric function which enters the Coulomb matrix element, any correlation beyond this is omitted. However, for an electron-hole plasma consisting of particle species with opposite charges, an important consequence of their mutual attraction is the existence of two-particle bound states, which are stable at least in a certain range of density and temperature. The purpose of the present paper is to extend the system of Boltzmann equations for electrons and holes by including similar equations for exciton populations, and to solve the coupled set through an ensemble Monte Carlo approach.

Excitonic effects are of major importance for the optical properties of pure direct semiconductors at low temperatures.¹⁸ Typical absorption spectra exhibit series of discrete lines below the gap energy which correspond to bound states of free excitons. The same lines are found in luminescence even when the excitation is at energies much higher than the band gap. If one assumes that under these conditions *free* electron-hole pairs are generated in the first place—which seems to be well justified for GaAs and similar III-V semiconductors¹⁹—it is clear that the excitonic *bound* states have to be populated afterwards simultaneously with the carrier relaxation.

The intrinsic process of exciton formation has been the subject of several experimental studies²⁰⁻²⁵ during recent years aiming to identify the mechanisms which are active in the buildup of an exciton population and, in particular, to determine characteristic times. Damen *et al.*²¹ have mea-

sured the time-resolved luminescence of high-quality GaAs/Al_{1-x}Ga_xAs quantum wells using an up-conversion technique. From an analysis of the temporal variation of the exciton line shape they concluded that bound states are formed with a time constant $\tau \leq 20$ ps in large-wave-vector states. The time required for the subsequent relaxation to optically active states within the homogeneous linewidth²⁶ Δ around $K=0$ by scattering with acoustic phonons is strongly temperature dependent and decreases from 400 ps at $T=5$ K to 20 ps at 60 K. The exciton distribution was found to be *nonthermal* during the entire time-interval of the measurements. These results were nearly independent of the laser excess energy in the range between 10 and 100 meV above the gap. Whereas it seems to be clear now that the binding of electron-hole pairs into excitons is a very fast process,²²⁻²⁵ there is less agreement about the dominant mechanism, which is attributed mainly to interaction with acoustic²¹ or with optical phonons.²⁴ Robart *et al.*²⁵ assume a thermodynamic equilibrium between excitons and free carriers at each time delay after the excitation and deduce a formation time ≤ 10 ps.

The concept behind the common interpretation of the experiments is that of rate equations for the densities of electrons, holes, and excitons which contain free parameters characterizing the different interactions (carrier generation, binding and dissociation of excitons, radiative free-carrier and excitonic recombination, etc.). These time constants are obtained by fits to the experimental data. Their definition, however, is not unique and different fitting procedures are used in the literature. Since this approach treats only particle densities, it implicitly assumes that the distribution functions are smooth, i.e., that the equilibration of the distributions is faster than any process contributing to the measured signal. The use of simple time constants implies further that the relevant microscopic transition probabilities have no strong dependence on the momenta of the particles involved. Both assumptions may be questioned and a microscopic kinetic theory of the coupled free-carrier and exciton relaxation is desired.

We address this problem by our system of coupled Boltzmann equations for electrons, holes, and excitons. We will confine ourselves to the low-density limit where screening of the exciton and other many-body complications like band-gap renormalization can be neglected. For an equilibrium system this would mean that the pair density has to be well below the Mott density which is, e.g., several 10^{15} cm^{-3} for GaAs at low temperatures.²⁷ The dominant mechanisms for the formation and dissociation of exciton bound states in this low-density regime are due to the interaction of the constituent electron-hole pairs with phonons. In the language of rate equations this corresponds to reaction terms which are simply proportional to the product of the electron and hole densities: $\propto Cnp$. The “bimolecular formation coefficient” C does depend on temperature but is density independent, which excludes Auger-like transitions. We will derive the probabilities for such transitions from the Hamiltonian of the exciton-phonon interaction using Fermi’s golden rule. They are used to set up collision integrals which couple the free-carrier and exciton distributions. The resulting system of rate equations in \vec{k} space is then solved by means of an ensemble Monte Carlo method. In our first implementation of the

method, we consider only the $1s$ exciton distribution.

We will treat as a first step bulk semiconductors; however, the general aspects of the kinetic theory outlined in this paper apply also to low-dimensional systems, on which most of the experiments have been performed. An application of our approach to GaAs quantum wells will be presented in a forthcoming publication.

The structure of the paper is the following. In Sec. II we outline our theoretical scheme: we introduce the kinetic equations for free carriers and excitons and the transition probabilities which enter as the main physical ingredients and couple the kinetic equations. The structure and energy dependence of the probabilities for exciton binding and dissociation are discussed in detail. After describing our numerical approach (Sec. III), in Sec. IV we show applications to bulk GaAs and present results for the buildup of an exciton population and its sensitivity to the excitation conditions (energy and density) and to temperature. The possibility of a selective tuning of exciton formation with laser energy is discussed in detail, together with its implications for luminescence experiments. Finally, Sec. V presents our view of the possible developments of our approach, including its application to low-dimensional semiconductors.

II. KINETIC THEORY

A. Kinetic equations for free carriers and excitons

In this section we will describe how the relaxation theory for optically generated electrons and holes can be extended to include free-moving aggregates of these particles which may form due to Coulomb attraction. The problem resembles in a certain sense that of a two-component plasma.²⁸ There are, however, important differences: The analogy between holes and positively charged ions is a rather formal one, and, moreover, it is of course important that the plasma is situated in a semiconductor and interacts with lattice vibrations. The description of two-particle bound states on a quantum mechanical level would require the treatment of suitable two-particle functions which contain just that part of the correlation which causes the binding. This could be done, e.g., in a density-matrix theory²⁹ by choice of an appropriate set of matrices and application of a decoupling scheme beyond the Hartree-Fock approximation. In fact, an extension of the semiconductor Bloch equations^{29,30} (SBE) has been given recently³¹ to describe the biexciton contribution to the nonlinear optical response of semiconductors. However, in a strict sense this theory treats properly coherent excitations only and damping is introduced phenomenologically. Thus, it is restricted to times during and just after the excitation. Although dephasing and scattering by carrier-carrier^{29,30} and by carrier-phonon¹⁶ interaction can be introduced into such a density-matrix theory on the single-particle level, this seems to be presently out of reach if two-particle correlations, and in particular bound states, have to be taken into account on a time scale up to hundreds of picoseconds, as in the relaxation regime.

We therefore take another point of view. Apart from details of the generation process itself, where the coherence of the excitation is essential and can be probed experimentally,³² the relaxation is satisfactorily described by a semiclassical theory which can be obtained from the SBE

TABLE I. Material parameters of the simplified GaAs model with two parabolic bands: the conduction and the heavy hole band.

Band gap E_g	1.519 eV
Electron effective mass m_e	$0.063m_0$
Hole effective mass m_h	$0.450m_0$
LO-phonon energy $\hbar\omega_0$	36.4 meV
Relative static dielectric constant κ_s	12.90
Relative optical dielectric constant κ_o	10.92
Crystal density ρ	5.37 g/cm^3
Longitudinal velocity of sound s	$5.33 \times 10^5 \text{ cm/s}$
Acoustic deformation potential (conduction band) D_e	7 eV
Acoustic deformation potential (valence band) D_h	-3.5 eV

by adiabatic elimination of the coherent interband polarization and Markov approximation. Assuming that the initial coherence and correlation of the generated electron-hole pairs is rapidly damped out (and, consequently, that the aforementioned approximations are reasonable), we will take the resulting Boltzmann equations for the particle distributions as the outset and complement them with similar equations for excitons as additional “particle species.”

Consider a simple bulk semiconductor model with two nondegenerate isotropic parabolic bands, the conduction band with dispersion $\epsilon_k^e = E_G + \hbar^2 k^2 / 2m_e$ and the valence band with $\epsilon_k^h = \hbar^2 k^2 / 2m_h$, respectively. m_e (m_h) is the effective mass of electrons (holes), and E_G is the gap energy. For practical calculations we will use parameters adapted to bulk GaAs, which are listed in Table I.

The single-particle states in this model are obviously plane waves. It is assumed that the system is homogeneous and that no external fields—apart from the light field of the exciting laser—are present. The system of coupled Boltzmann equations for the distribution functions of both free-particle species may then be formally written as

$$\frac{d}{dt} f_e(\vec{k})|_{fp} = G_{\vec{k}}(t) + \sum_i \frac{d}{dt} f_e(\vec{k})|_i, \quad (2.1)$$

$$\frac{d}{dt} f_h(\vec{k})|_{fp} = G_{-\vec{k}}(t) + \sum_i \frac{d}{dt} f_h(\vec{k})|_i. \quad (2.2)$$

The first term on the right-hand side of both equations is a time-dependent optical generation rate, $G_{\vec{k}}(t)$. The appearance of the same function $G_{\vec{k}}(t)$ in both kinetic equations accounts for the fact that electrons and holes are generated always pairwise and with opposite momenta due to the vanishing wave vectors of the incident photons. We will specify the explicit form of $G_{\vec{k}}(t)$ later.

The second contributions to the temporal change of the distribution functions are collision integrals which describe particle scattering due to the various interaction mechanisms denoted by the superscript i . Their general structure ($s = e, h$),

$$\begin{aligned} \frac{d}{dt} f_s(\vec{k})|_i = & \sum_{\vec{k}'} \{ W_s^i(\vec{k}, \vec{k}') f_s(\vec{k}') [1 - f_s(\vec{k})] \\ & - W_s^i(\vec{k}', \vec{k}) f_s(\vec{k}) [1 - f_s(\vec{k}')] \}, \end{aligned} \quad (2.3)$$

is easily understood as the net change of occupation of the state \vec{k} due to the balance of the gain by in-scattering from all available states, \vec{k}' , and the reverse process of out-scattering.³³ The Pauli blocking factors in (2.3) are written for completeness; they have no practical relevance in the low-density regime that we will consider. The probabilities of the microscopic transitions are given by the $W_s^i(\vec{k}, \vec{k}')$. In second-order perturbation theory and Markovian approximation they are obtained from Fermi's golden rule and ensure conservation of energy and momentum. The explicit expressions for electron-phonon scattering read:

$$\begin{aligned} W_s^i(\vec{k} + \vec{q}, \vec{k}) = & \frac{2\pi}{\hbar} \sum_{\pm} |C_{s,q}^i|^2 (n_{\vec{q}} + \frac{1}{2} \pm \frac{1}{2}) \\ & \times \delta(\epsilon_{\vec{k}+\vec{q}}^s - \epsilon_{\vec{k}}^s \pm \hbar\omega_{\vec{q}}), \end{aligned} \quad (2.4)$$

where the upper sign refers to emission and the lower one to absorption. $n_{\vec{q}}$ is the occupation number of a phonon mode with wave vector \vec{q} and energy $\hbar\omega_{\vec{q}}$, which is the Bose function if deviations of the phonon system from equilibrium can be neglected, as in the present case.

The coupling constants $C_{s,q}^i$ specify the interaction of particles and lattice vibrations. We will consider the Fröhlich interaction with LO phonons of frequency ω_0 where

$$|C_{e,q}|^2 = |C_{h,q}|^2 = \frac{2\pi e^2}{\Omega} \hbar\omega_0 \left(\frac{1}{\kappa_o} - \frac{1}{\kappa_s} \right) \frac{1}{q^2} \quad (2.5)$$

(κ_o and κ_s are the high- and low-frequency dielectric constants) and the deformation-potential coupling to acoustic phonons in isotropic approximation with

$$|C_{s,q}|^2 = \frac{\hbar}{2\rho v \Omega} D_s^2 q (s = e, h) \quad (2.6)$$

(D_s is the deformation potential, ρ the crystal density, and v the velocity of sound). Ω is a normalization volume.

The transition probabilities for carrier-carrier scattering, which depend on the distribution functions even for the non-degenerate case, are written as

$$\begin{aligned} W_s(\vec{k} + \vec{q}, \vec{k}) = & \frac{2\pi}{\hbar} \sum_{s'=e,h} \sum_{\vec{k}'} |V_q|^2 f_{s'}(\vec{k}') [1 - f_{s'}(\vec{k}' - \vec{q})] \\ & \times \delta(\epsilon_{\vec{k}+\vec{q}}^s + \epsilon_{\vec{k}'}^{s'} - \epsilon_{\vec{k}}^s - \epsilon_{\vec{k}'-\vec{q}}^{s'}) \end{aligned} \quad (2.7)$$

with V_q being the matrix element of the screened Coulomb interaction.

Kinetic equations for excitons³⁴ may be set up along the same lines, starting from an appropriate set of basis functions: the eigensolutions of the stationary two-particle Schrödinger equation of an electron-hole pair interacting via statically screened Coulomb attraction, which in effective-mass approximation reads:

$$\left[-\frac{\hbar^2}{2m_e}\Delta_e - \frac{\hbar^2}{2m_h}\Delta_h - \frac{e^2}{\kappa_s |\vec{r}_e - \vec{r}_h|} \right] \Psi(\vec{r}_e, \vec{r}_h) = E \Psi(\vec{r}_e, \vec{r}_h). \quad (2.8)$$

Apart from the simplifications in the band-structure model, this equation describes a highly idealized system of just two interacting particles and has to be seen as a low-density limit of a much more complicated many-body problem. We will confine ourselves to this regime where corrections due to phase-space filling, density-dependent screening, and band-gap renormalization can be ruled out.

Transforming to center-of-mass (COM) and relative coordinates

$$\vec{R} = \frac{m_e \vec{r}_e + m_h \vec{r}_h}{(m_e + m_h)}, \quad \vec{r} = \vec{r}_e - \vec{r}_h,$$

the wave function is readily factorized as

$$\Psi(\vec{R}, \vec{r}) = \frac{1}{\sqrt{\Omega}} e^{i\vec{K}\vec{R}} \Phi_{\nu}(\vec{r}) \quad (2.9)$$

(Ω is the normalization volume). The plane-wave factor describes the free motion of the COM of the aggregate through the crystal. Solutions of the remaining hydrogenlike problem for the relative wave function $\Phi_{\nu}(\vec{r})$ are well known³⁵ for both bound and continuum states.

In the former case, ν stands for a set of discrete quantum numbers. The eigenenergies of bound states with principal quantum numbers $n=1, 2, \dots$ are given by the familiar expression

$$\epsilon_{\vec{K}}^{\nu} = E_G - \frac{\varepsilon_0}{n^2} + \frac{\hbar^2 K^2}{2M}, \quad (2.10)$$

with $\varepsilon_0 = e^4 \mu / 2 \kappa_s^2 \hbar^2$ being the effective Rydberg ($\mu^{-1} = m_e^{-1} + m_h^{-1}$ is the reduced mass). Our model yields the numerical value of $\varepsilon_0 = 4.2$ meV; the corresponding Bohr radius is $a_0 = \hbar^2 \kappa_s / e^2 \mu = 136$ Å. Equation (2.10) is the dispersion of free particles with wave vector \vec{K} in parabolic bands of mass $M = m_e + m_h$; bands with identical principal quantum numbers are degenerate. One can label the bound exciton states by “band indices” ν and wave vectors \vec{K} (which reads in a bracket notation $|\nu, \vec{K}\rangle$) and treat them as composite particles with internal degrees of freedom. For the distribution functions of these additional particle species, $f_{\nu}(\vec{K})$, we may set up semiclassical kinetic equations analogous to (2.3):

$$\begin{aligned} \frac{d}{dt} f_{\nu}(\vec{K}) = & \sum_{\nu' \vec{K}'} [\mathcal{W}_{\nu\nu'}^i(\vec{K}, \vec{K}') f_{\nu'}(\vec{K}') \\ & - \mathcal{W}_{\nu'\nu}^i(\vec{K}', \vec{K}) f_{\nu}(\vec{K})]. \end{aligned} \quad (2.11)$$

We have not included a generation rate for excitons since we are interested in off-resonant excitation which produces e - h pairs with small momenta in the continuum. Generation of “hot excitons”³⁶ is possible only via assisted interband transitions where a partner particle (e.g., a phonon) provides the necessary momentum to reach bound states with large \vec{K} . Such processes could be taken into account easily but for simplicity we will assume that they are negligible. The transition probabilities in (2.11) will be considered explicitly in the next subsection.

Eigenstates belonging to positive energy eigenvalues for the relative motion form a continuum and may be labeled by \vec{K} and a relative momentum \vec{p} . Their dispersion

$$\epsilon_{\vec{p}}(\vec{K}) = E_G + \frac{\hbar^2 K^2}{2M} + \frac{\hbar^2 p^2}{2\mu} = E_G + \frac{\hbar^2 k_e^2}{2m_e} + \frac{\hbar^2 k_h^2}{2m_h} \quad (2.12)$$

is identical to that of noninteracting electron-hole pairs as can be seen by insertion of the definitions

$$\vec{K} = \vec{k}_e + \vec{k}_h, \quad \vec{p} = \beta \vec{k}_e - \alpha \vec{k}_h,$$

where we have introduced the mass factors $\alpha = m_e/M$ and $\beta = m_h/M$. The relative wave functions $\Phi_{\vec{p}}(\vec{r})$, and consequently the oscillator strengths for optical transitions, differ from the free-particle result (“Sommerfeld enhancement” of continuum absorption³⁷). However, to keep the connection to the kinetic description of the free carriers in terms of the Boltzmann equations, we will approximate the continuum states as products of plane waves and neglect their Coulomb correlation. From now on we will call bound exciton states simply “excitons” and continuum states “free carriers.”

B. Exciton-phonon interaction and transitions between bound states

The interaction of Wannier excitons with phonons has been treated in the literature for the case of bulk semiconductors³⁸ as well as for quantum well structures.³⁴ The corresponding Hamiltonian is simply obtained by calculating matrix elements of the sum of the electron-phonon and hole-phonon interaction Hamiltonians between suitable exciton states. For scattering between the bound states $|\nu, \vec{K}\rangle$ introduced above the result reads:

$$H_{\text{ex-ph}}^i = \sum_{\vec{K}, \vec{q}} \sum_{\nu, \nu'} D_{\nu\nu'}^i(\vec{q}) |\nu', \vec{K} + \vec{q}\rangle \langle \nu, \vec{K} | (b_{i,-\vec{q}}^{\dagger} + b_{i,\vec{q}}). \quad (2.13)$$

$b_{i,\vec{q}}^{\dagger}$ and $b_{i,\vec{q}}$ are the creation and annihilation operators of phonon modes with wave vector \vec{q} ; the index i labels, as before, a certain branch of the phonon dispersion and the interaction mechanism. The \vec{q} -dependent effective coupling constant $D_{\nu\nu'}^i(\vec{q})$ is the weighted sum of the individual coupling constants of electrons and holes:

$$D_{\nu\nu'}^i(\vec{q}) = C_{e,q}^i S_{\nu\nu'}(\beta\vec{q}) - C_{h,q}^i S_{\nu\nu'}(-\alpha\vec{q}) \quad (2.14)$$

(the minus sign stems from the transformation to the electron-hole picture). The weights in (2.14) are the exciton form factors:

$$S_{\nu\nu'}(\vec{q}) = \int d^3r \Phi_{\nu'}^*(\vec{r}) e^{i\vec{q}\cdot\vec{r}} \Phi_{\nu}(\vec{r}), \quad (2.15)$$

which are Fourier transforms of the products of relative wave functions of the states involved in the transition. Note that for different free-particle masses, $\alpha \neq \beta$, electrons and holes contribute differently to the probability (and charge) density distribution of the exciton and, consequently, to the response to a certain phonon mode.

If both the initial and final state are in the lowest exciton band, one obtains explicitly from the ground state wave function

$$\Phi_0(\vec{r}) = \frac{1}{\sqrt{\pi a_0^3}} e^{-r/a_0} \quad (2.16)$$

the well-known result

$$S_{00}(\vec{q}) = \frac{1}{[1 + (qa_0/2)^2]^2}. \quad (2.17)$$

Similar expressions are easily derived for other combinations of bands ν and ν' .

The transition probabilities in lowest-order perturbation theory with respect to $H_{\text{ex-ph}}$,

$$\begin{aligned} \mathcal{W}_{\nu\nu'}^i(\vec{K} + \vec{q}, \vec{K}) &= \frac{2\pi}{\hbar} \sum_{\pm} |D_{\nu\nu'}^i(\vec{q})|^2 \left(n_{\vec{q}} + \frac{1}{2} \pm \frac{1}{2} \right) \\ &\times \delta(\epsilon_{\vec{K}+\vec{q}}^{\nu'} - \epsilon_{\vec{K}}^{\nu} \pm \hbar\omega_{\vec{q}}), \end{aligned} \quad (2.18)$$

are, of course, similar to the free-carrier ones (2.4). Integration of $\mathcal{W}_{\nu\nu'}^i(\vec{K} + \vec{q}, \vec{K})$ over the final states yields the scattering rate

$$\Gamma_{\nu\nu'}^i(\vec{K}) = \sum_{\vec{q}} \mathcal{W}_{\nu\nu'}^i(\vec{K} + \vec{q}, \vec{K}), \quad (2.19)$$

which is proportional to the inverse lifetime of state $|\nu, \vec{K}\rangle$ due to process i and depends, for a homogeneous system, only on $|\vec{K}|$. In Fig. 1 we have plotted the scattering rates for several transitions involving states in the $1s$ exciton band at $T=4.2$ K. Figure 1(a) shows the rates for scattering within the lowest exciton band and to the next higher $2s$ and $2p$ bands under emission of LO phonons (absorption of optical phonons can be neglected at these low temperatures). The intraband scattering rate reaches a maximum value of $\approx 5 \text{ ps}^{-1}$ which is close to the corresponding value for electrons: the effect of the larger exciton mass M , which would increase the rate, is nearly compensated by the reduction due to the form factor. The scattering to higher exciton bands is less effective by at least an order of magnitude (this holds also for all other transitions to bound states not shown here).

Luminescence is dominantly emitted from the lowest exciton band since only states with s symmetry, i.e., zero angular momentum, are involved in dipole-allowed transitions

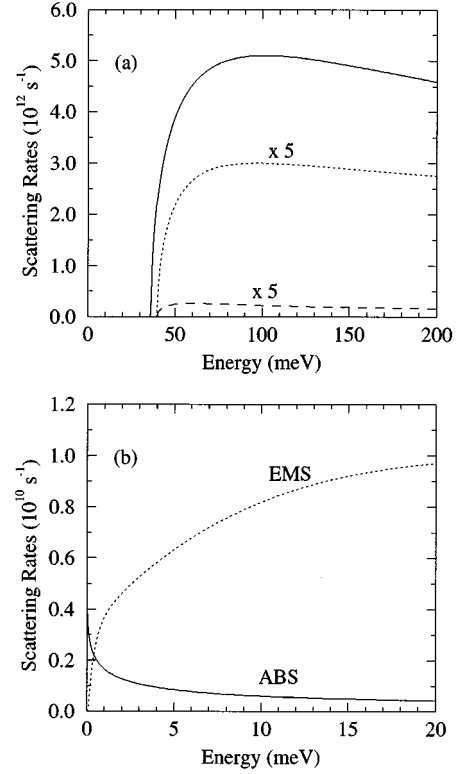


FIG. 1. Scattering rates for transitions between exciton bound states at $T=4.2$ K. (a) Transitions under emission of LO phonons within the $1s$ band (solid line), and from $1s$ to the $2s$ (dashed), and to the $2p$ (dotted) bands, respectively. The latter two curves have been scaled by a factor of 5. (b) Inelastic scattering within the $1s$ band by emission (upper curve) and absorption (lower curve) of acoustic phonons via the deformation-potential coupling. Note the different scales.

and their oscillator strengths scale with the principal quantum number as n^{-3} in a bulk system.¹⁸ For this reason and because the transfer of excitons between the ground state and excited states by phonon scattering is slow compared to the intraband processes, we will confine ourselves to the $1s$ exciton distribution, which is labeled $f_X(\vec{K})$.

Deformation-potential scattering [Fig. 1(b)] is even slower than the interaction with LO phonons. Nevertheless, it turns out to be important since it is the only relaxation mechanism for energies below the optical-phonon energy $\hbar\omega_0=36.4$ meV. It has to be expected that these processes which redistribute excitons from large-wave-vector states to the optically active states in the vicinity of $K=0$ take place on a time scale of hundreds of picoseconds.

C. Reaction terms and coupling of the kinetic equations

The most important physical processes that couple the distributions of free carriers and excitons are binding and dissociation: an e - h pair in the continuum undergoes a transition into a bound state, and vice versa. Due to energy and momentum conservation, these processes have to be assisted by some partner particle. For low densities—the situation we are interested in—it can be assumed that phonon-mediated transitions will dominate. In analogy to a chemical reaction we express them formally as

$$e + h \rightleftharpoons X, \quad (2.20)$$

and presuppose that the rates of these reactions will be proportional to the product of the electron and hole densities for binding and proportional to the exciton density for dissociation with a density-independent constant of proportionality C . This is exactly the idea behind the rate-equation concept: it is assumed that all particles of a given species contribute to the reactions, at least on average, in the same way. In other words, both the distribution functions and the transition probabilities should have a smooth dependence on the microscopic state variables, i.e., on the particle momenta. On the other hand, it is well known that optical excitation high in the bands generates distribution functions in strong nonequilibrium, which are very structured at the beginning of the relaxation process.

Therefore, we are led to give a transcription of Eq. (2.20) on a kinetic level which is consistent with the Boltzmann equations (2.3). If R^B and R^D are the binding and dissociation probabilities, we make the following *ansatz* for the reaction terms in the kinetic equations which guarantees conservation of the total number of e - h pairs, bound and free, in the system:

$$\begin{aligned} \frac{d}{dt} f_e(\vec{k}_e)|_R &= \sum_{\vec{k}_h, \vec{K}} [R^D(\vec{k}_e, \vec{k}_h; \vec{K}) f_X(\vec{K}) \\ &\quad - R^B(\vec{K}; \vec{k}_e, \vec{k}_h) f_e(\vec{k}_e) f_h(\vec{k}_h)], \\ \frac{d}{dt} f_h(\vec{k}_h)|_R &= \sum_{\vec{k}_e, \vec{K}} [R^D(\vec{k}_e, \vec{k}_h; \vec{K}) f_X(\vec{K}) \\ &\quad - R^B(\vec{K}; \vec{k}_e, \vec{k}_h) f_e(\vec{k}_e) f_h(\vec{k}_h)], \quad (2.21) \\ \frac{d}{dt} f_X(\vec{K})|_R &= \sum_{\vec{k}_e, \vec{k}_h} [R^B(\vec{K}; \vec{k}_e, \vec{k}_h) f_e(\vec{k}_e) f_h(\vec{k}_h) \\ &\quad - R^D(\vec{k}_e, \vec{k}_h; \vec{K}) f_X(\vec{K})]. \end{aligned}$$

The binding contribution, representing a gain term for the occupation $f_X(\vec{K})$ of state \vec{K} in the exciton band, is set proportional to the distribution functions of electrons and holes. The loss term describing dissociation, in turn, depends only on the exciton distribution. In accordance with our central assumption of low particle densities and the neglect of many-body aspects in the description of the exciton states, we have omitted here and in Eq. (2.11) any occupation factors of the final states which would describe quantum corrections.

The microscopic transition probabilities R^B and R^D are again obtained in lowest-order perturbation theory with respect to the Hamiltonian of the exciton-phonon interaction, now using free e - h pair states $|\vec{p}, \vec{K}\rangle = |\vec{k}_e, \vec{k}_h\rangle$ as initial or final states. Let us consider explicitly binding transitions which are possible under emission or absorption of a phonon; the corresponding probability is expressed as (upper sign: emission)

$$\begin{aligned} R_{\pm}^B(\vec{K}; \vec{k}_e, \vec{k}_h) &= \frac{2\pi}{\hbar} \sum_q |\tilde{D}^i|^2 \left(n_{\vec{q}} + \frac{1}{2} \pm \frac{1}{2} \right) \delta_{\vec{K} \pm \vec{q}, \vec{k}_e + \vec{k}_h} \\ &\quad \times \delta(\epsilon_{\vec{K}}^X - \epsilon_{\vec{k}_e}^e - \epsilon_{\vec{k}_h}^h \pm \hbar \omega_q). \end{aligned} \quad (2.22)$$

Apart from the fact that we have written the conservation law for the COM momentum explicitly here (the relative momentum is *not* conserved), this is formally analogous to Eq. (2.18). The effective coupling constant \tilde{D}^i can be expressed again as a sum of an electron and a hole contribution:

$$\tilde{D}^i = C_{e\vec{q}}^i S_X [\beta(\vec{k}_e + \vec{q}) - \alpha \vec{k}_h] - C_{h\vec{q}}^i S_X [\beta \vec{k}_e - \alpha(\vec{k}_h + \vec{q})] \quad (2.23)$$

with a form factor S_X that measures the overlap of the exciton $1s$ wave function with the plane-wave states in the continuum:

$$S_X(\vec{q}) = \left(\frac{(2a_0)^3 \pi}{\Omega} \right)^{1/2} \frac{1}{[1 + (qa_0)^2]^2}. \quad (2.24)$$

As they stand, the binding probabilities R_{\pm}^B are complicated functions of the momenta of the particles involved in the transitions. However, some of the information they contain is redundant. The distribution functions of the three particle species will depend only on the absolute values of their arguments at any instant of time in an isotropic system. Furthermore, for given k_e and k_h , the possible final exciton COM momenta K are completely fixed by the conservation laws in Eq. (2.22). Thus, we can perform the summation over the phonon wave vector \vec{q} in R_{\pm}^B , sum over the possible final exciton states \vec{K} , and integrate out the ‘‘unnecessary’’ angle between the initial electron and hole wave vectors:

$$R_{\pm}^B(\vec{K}; \vec{k}_e, \vec{k}_h) \rightarrow \Gamma_{\pm}^B(k_e, k_h).$$

$\Gamma_{\pm}^B(k_e, k_h)$ is a scattering rate for phonon-assisted transitions of an e - h pair into a bound state in the $1s$ exciton band.

The result for the most efficient exciton formation mechanism in our model system, binding under emission of one LO phonon, is shown in Fig. 2 as a function of the electron and hole energies. Multiplication of this function with the particle distribution functions including appropriate normalization factors (and with $n_{\vec{q}} + 1$) and integration over the initial particle momenta according to Eqs. (2.21) yields directly the rate of exciton binding or, in other words, the rate of ‘‘loss’’ of free pairs in the continuum. The pronounced structures result from two causes. First, it is clear that energy conservation according to Fermi’s golden rule requires that the e - h pair in the initial state has to have a minimum energy to be able to emit an optical phonon with a final state in the exciton band. Since the edge of the exciton band is *below* the continuum by just the amount of the exciton binding energy ε_0 , this threshold is at $\hbar \omega_0 - \varepsilon_0$. The sharp peaks just above the threshold and the rapid decrease of the scattering rate for higher particle, in particular electron, energies are due to the polar nature of the Fröhlich interaction and, even more, due to the strong wave-vector dependence of the form factor S_X . The apparent asymmetry with respect to the particle energies is again due to the different polarizabilities of the electron and hole contributions to the exciton charge density

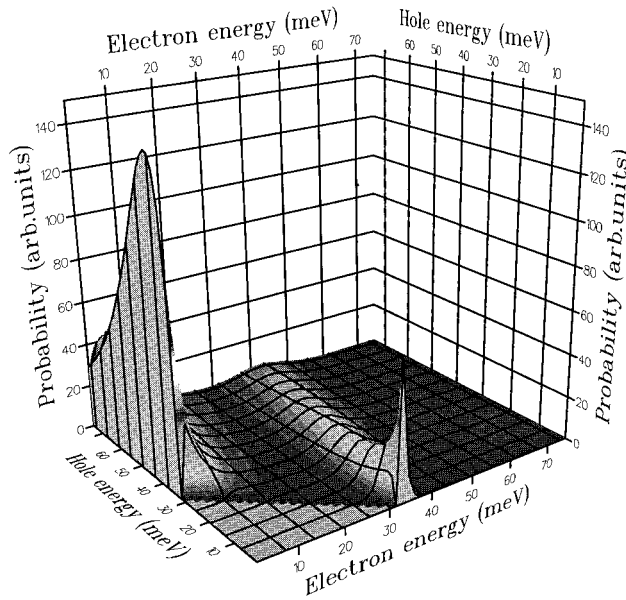


FIG. 2. Integrated transition probability for the formation of excitons under emission of one LO phonon as a function of the electron and hole energies.

($m_e \neq m_h$). Transitions where basically the entire necessary energy is provided by one of the free carriers are favored.

Figure 3 gives the result of the similar calculation for the rate of dissociation under absorption of a LO phonon, $\Gamma^D(K, k_h)$, as a function of the initial exciton energy and the energy of the final hole state (the energy of the released electron follows from the conservation law). This process is active at high enough temperatures when sufficient phonon modes are occupied according to the Bose distribution n_q . The two “ribs” in the plane with nonvanishing values of the rate again correspond to transitions where practically all of

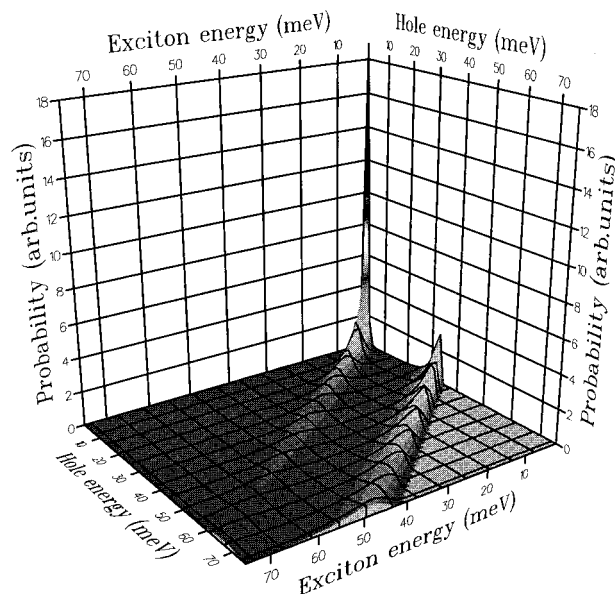


FIG. 3. Integrated transition probability for the dissociation of excitons under absorption of one LO phonon as a function of the electron and hole energies.

the initial energy, i.e., the initial exciton energy plus that of the absorbed phonon, is gained by either the electron or the hole. Their different weights are determined by the form factors: hole states of a given energy are at much larger wave vectors than electron states with the same energy.

At this point some remarks about our approximations are in place. The Markovian approximation, i.e., the use of Fermi's golden rule with strict conservation laws for energy and momentum, is the basis of any semiclassical kinetic theory in terms of Boltzmann equations. Apart from this, we have used simple plane waves for the continuum states in the calculation of the transition rates and left out Coulomb correlation in that part of the spectrum. As already mentioned, this is consistent with the treatment of the free-carrier kinetics, and it is expected that the various scattering processes present in the system damp out the coherence of the e - h pair. There are, however, situations where the scattering states have to be treated as solutions of the Coulomb problem, e.g., for the description of second-order Raman scattering.³⁹ Rudin *et al.* have calculated the phonon contribution to the exciton linewidth using Coulomb scattering states in Fermi's golden rule approach for several bulk semiconductors⁴⁰ and quantum well systems.⁴¹ For the latter they have compared their results with previous⁴² ones and have found differences by a factor of the order of 2. The LO-phonon-induced linewidth of the exciton due to transitions into the continuum can be obtained from the dissociation probability for the exciton momentum $K=0$ (see Fig. 3) by integration over the final hole states. Writing it as proportional to the phonon occupation number n_q , $\Delta_{1s,cont}^{LO} = \gamma_{1s,cont}^{LO} n_q$, a temperature-independent linewidth parameter $\gamma_{1s,cont}^{LO}$ is defined. Using the material parameters of Ref. 40, our calculation gives $\gamma_{1s,cont}^{LO} = 9$ meV whereas the (corrected) value of Rudin *et al.* is 4.21 meV. An estimate of the result of the approximation under consideration in the general case (for arbitrary combinations of particle momenta) is difficult and further work, both conceptual and practical, is needed.

III. NUMERICAL METHOD

A. Ensemble Monte Carlo technique

The complete system of kinetic equations is now written as

$$\frac{d}{dt}f_s(\vec{k}) = \frac{d}{dt}f_s(\vec{k})|_{fp} + \frac{d}{dt}f_s(\vec{k})|_R \quad (s=e, h, X). \quad (3.1)$$

This is a set of Markovian rate equations in \vec{k} space and may be solved by means of a Monte Carlo simulation. This technique allows for the inclusion of different, even complicated, scattering mechanisms and provides a clear and intuitive picture of the physical system.⁴³ In general, it consists in modeling the processes which change a particle's state in time (free flights and random scattering events) stochastically, according to the known transition probabilities, and in calculating suitable statistical averages.

For linear ergodic systems it suffices in principle to simulate a single particle: the ensemble average can be replaced by a time average. The solution of nonlinear problems where the time-dependent distribution functions have to be known

in order to calculate the scattering rates requires the simulation of particle ensembles. This is already the case when the Pauli principle is included and, of course in the presence of particle-particle interactions. The accuracy of such a simulation will then depend on the ensemble size.⁴⁴ An efficient way to handle very large numbers of particles is based on phase-space discretization⁴⁵ and the introduction of an “occupation number representation”.^{16,}

We use the fact that in our isotropic system all functions of the wave vector \vec{k} depend only on its absolute value k and introduce an equidistant discretization with step size Δk between $k=0$ and some k_{\max} . In this way we define “cells” around certain points k_i which contain all k with

$$k_i - \frac{1}{2} \Delta k \leq k < k_i + \frac{1}{2} \Delta k;$$

the distribution functions are approximated as stepwise constant. The total number of available states in band λ for each cell, ν_λ^i , has to be determined from the density of states (per band) in \vec{k} space, which is $\Omega/4\pi^3$ for a three-dimensional (spin-degenerate) system of volume Ω . Accordingly, the number of states $d\nu_\lambda^i$ in an infinitesimal spherical shell of thickness dk around k_i is given by

$$d\nu_\lambda^i = \frac{\Omega}{\pi^2} k_i^2 dk$$

and integration of this relation yields ν_λ^i . The normalization volume Ω has to be fixed by $n_\lambda = N_\lambda^s/\Omega$, which relates the total number of *simulated* particles N_s to their *physical* density n_λ in one particular band; the number of particles in the other bands is calculated with the given Ω from their densities.

This phase-space discretization has several advantages compared to ensemble Monte Carlo (EMC) methods which follow the trajectories of individual particles characterized by their wave vectors $\vec{k}_i(t)$. First of all, as the ratio of the number of particles present in a cell at a time t to the number of states available in it is naturally interpreted as an average occupation number

$$f_\lambda^i(t) = \frac{N_\lambda^i(t)}{\nu_\lambda^i},$$

the method gives direct access to the distribution functions at any instant. Scattering of a particle between different \vec{k} states means simply reducing N_λ^i in 1 cell and increasing it in another just by one. The Pauli exclusion principle can be fulfilled, if needed, by a trivial rejection technique which compares a uniformly distributed random number (on the unit interval) with the occupation factor $[1 - f_\lambda^i(t)]$. From a computational point of view it is advantageous that the memory required to store the necessary information about the actual state of the system does not depend on the number of simulated particles but only on that of the cells, which is typically several hundreds. In this way we are able to work easily with as many as several hundred thousand particles. The size of the ensemble is limited only by computer time.

The simulation itself consists of a sequence of time steps of equal duration δt up to the desired total simulation time. For $t=t_0$ before the laser excitation we define initial condi-

tions for the system which may be either in the ground state, corresponding to vanishing $f_s(k)$ for all k , or in any other state with predefined isotropic, e.g., thermal, distributions. The time-dependent rates for carrier-carrier scattering and exciton reactions are then updated at the beginning of each time step t_i , using the known distribution functions. Obviously, δt has to be chosen small enough to allow for the neglect of any time variation in the nonlinear contributions entering our kinetic equations. During the time steps a conventional Monte Carlo procedure is applied to every particle: the physical processes which may change their state—optical generation and scattering—are modeled using random num-

B. Exciton transitions

The MC treatment of free-carrier scattering is standard,^{43,44} that of exciton intraband transitions is identical since the collision integral for these processes (2.11) has the same structure as the free-carrier one (2.3) in the nondegenerate limit. The only change is the appearance of the exciton form factor in the matrix element.

Exciton reactions are many-particle collisions involving free carriers, excitons, and phonons. For transitions into bound states the scattering rate for the pair states, $\Gamma_\pm^B(k_e, k_h)$, is multiplied with the distribution function of particle species j and integrated over the wave vector k_j :

$$p_\pm^B(k_i) = \sum_{k_j} \Gamma_\pm^B(k_i, k_j) f_j(k_j). \quad (3.2)$$

This yields a time-dependent scattering probability $p_\pm^B(k_i)$ for the other species i , which can be used in the common way to choose the scattering mechanism according to its probability and to determine the time of free flight, and has to be updated for every time step. The final state K and the wave vector of the participating phonon are chosen according to the conservation laws and the implicit probability distribution given by $R_\pm^B(\vec{K}, \vec{k}_e, \vec{k}_h)$. The contribution of dissociation to the reaction terms (2.21) is proportional to the exciton distribution $f_X(K)$ alone. The transition probabilities R_\pm^D can be integrated over both free-carrier momenta, which results in a “conventional” scattering rate $p_\pm^D(K)$ for the dissociation of an exciton in state K . The function R_\pm^D , however, is needed for the choice of the final state of the pair.

IV. APPLICATIONS

Simulations have been performed for a two-band model with GaAs-like parameters (see Table I). The exciting laser pulses are taken as Gaussians with central frequency ω_L and width τ_L , centered at $t=0$:

$$E(t) = E_0 \exp\left[-\frac{t^2}{\tau_L^2}\right]; \quad (4.1)$$

for all calculations presented here we use a pulse duration of $\tau_L = 500$ fs. From (4.1) one obtains approximately¹⁶ the semiclassical generation rate:

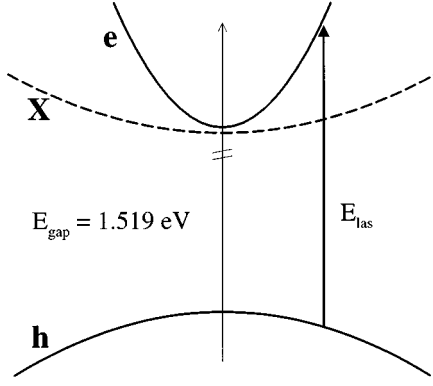


FIG. 4. Schematic representation of optical transitions (absorption). Conduction band (e), valence band (h), and the $1s$ exciton band (X) are shown. The gap energy at $T=0$ is 1.519 eV in the model.

$$G_{\vec{k}}(t) = \sqrt{2\pi} \left[\frac{\mu_{\vec{k}} E_0}{\hbar} \right]^2 \tau_L \exp \left[-\frac{2t^2}{\tau_L^2} \right] \exp \left[-\frac{1}{2} \Omega_k^2 \tau_L^2 \right] \times [1 - f_e(\vec{k}) - f_h(-\vec{k})] \quad (4.2)$$

with $\mu_{\vec{k}}$ being the dipole matrix element and $\hbar\Omega_k = \hbar\omega_L - (\epsilon_{\vec{k}}^e + \epsilon_{-\vec{k}}^h)$. Since the pulse width is finite the pair energies are spread around $\hbar\omega_L$ and (4.2) can be seen as proportional to their (Gaussian) distribution. For practical purposes we rewrite it (neglecting the \vec{k} dependence of $\mu_{\vec{k}}$) as

$$G_{\vec{k}}(t) = n_0 \sqrt{\frac{2}{\pi \tau_L^2}} \exp \left[-\frac{2t^2}{\tau_L^2} \right] \exp \left[-\frac{1}{2} \Omega_k^2 \tau_L^2 \right] \times [1 - f_e(\vec{k}) - f_h(-\vec{k})]$$

and set the final pair density n_0 , i.e., the total density of e - h pairs generated by the pulse, to its desired value.

The elementary process of optical excitation is schematically depicted in Fig. 4: the transition that generates an electron in the conduction band and leaves a hole in the valence band is vertical in \vec{k} space since the momentum of the incident photon can be neglected in practice. This means, obviously, that the excess energy of the laser beam, $\Delta E = \hbar\omega - E_G$, is shared asymmetrically between electron and hole for different effective masses in the two bands. The major part, $\Delta E/(1 + m_e/m_h)$, is transferred to the electron (for our parameters this is $\approx 0.88\Delta E$). Thus, for experimentally relevant excess energies up to, say, ≈ 200 meV (well below the upper L valleys in the conduction band of GaAs), the initial energy of the photoexcited holes will always be lower than the LO-phonon energy and their relaxation will be determined by carrier-carrier and acoustic-phonon scattering. On the other hand, the mean energy of the initial electron distribution can be chosen everywhere in this range by tuning the laser excess energy ΔE . In particular, it is possible to generate electrons selectively at energies where the probability of LO-phonon-assisted exciton formation is large (see Fig. 2).

A. Sensitivity of exciton formation to the excitation conditions

Results of a simulation for this case are shown in Fig. 5. The initial peak of the electron distribution [Fig. 5(b)] is centered at ≈ 30 meV, a large fraction of particles being in states with a high probability for transitions into exciton states under emission of one LO phonon. This very fast process starts already during the laser pulse and after 5 ps [lowest curve in Fig. 5(a)] a substantial exciton population with center at 3 meV is established. For longer times it piles up further and relaxes much more slowly towards the edge of the $1s$ band by inelastic deformation-potential scattering. As time elapses the peak in the electron distribution, Fig. 5(b), is broadened, mainly by carrier-carrier interaction, and slowly transferred to lower energies. The fastest possible relaxation mechanism, intraband emission of LO phonons, is operative only for electrons above $\hbar\omega_0$, and the energy range with high formation probability remains well occupied for rather long times up to 50 ps. The time dependence of the hole distribution, Fig. 5(c), is, as expected, determined by frequent carrier-carrier scattering (broadening) and interaction with acoustic phonons (relaxation). For all times the holes remain at low energies, and the efficiency of the exciton formation depends on the shape of the *electron* distribution alone. These results have been obtained for a final pair density of $n_0 = 10^{14} \text{ cm}^{-3}$ and lattice temperature of $T = 4.2$ K. The total exciton density n_X reaches monotonically $\approx 1.7 \times 10^{13} \text{ cm}^{-3}$ after 200 ps, which is practically its asymptotic value. In Fig. 5(d) we compare the time evolution of n_X for the same laser energy and intensity but different temperatures. Above ≈ 50 K exciton dissociation gains importance, which is mainly due to LO-phonon absorption and thus is weighted by the Bose occupation factor. In an intermediate range of temperatures the initial binding is much faster than the dissociation, and an overshooting of n_X over its asymptotic value is found. At higher temperatures⁴⁷ a stationary value, which is lower by nearly an order of magnitude than that for 4.2 K, is reached much faster: excitons dissociate as fast as they bind. The deformation-potential coupling of excitons is, as for free carriers, much weaker than the Fröhlich interaction. The contribution of this mechanism to transitions between bound and continuum states is not important on the present time scale up to 200 ps. Nevertheless, it is responsible for the energy loss within the $1s$ band.

For the results discussed so far it was essential that electrons were generated in a region in \vec{k} space where transitions into excitons are favored. For simplicity, we will call this kind of excitation “resonant” (RE), which should not be confused with direct excitation of excitons at $K=0$. Tuning the laser, it is possible to excite “off resonantly” (ORE) as well: the excess energy is chosen such that the initial electron distribution peaks at energies where the binding probability is low. This condition is fulfilled for the simulation presented in Fig. 6 with $\Delta E = 68$ meV. The electrons are generated around 60 meV but are immediately (within ≈ 0.3 ps) scattered into the first LO-phonon satellite. This is the structure around 24 meV at 5 ps after the pulse in Fig. 6(b). It is now *below* the threshold for exciton binding, and the only particles that can be scattered into bound states are those of the high-energy tail that emerges at later times, due

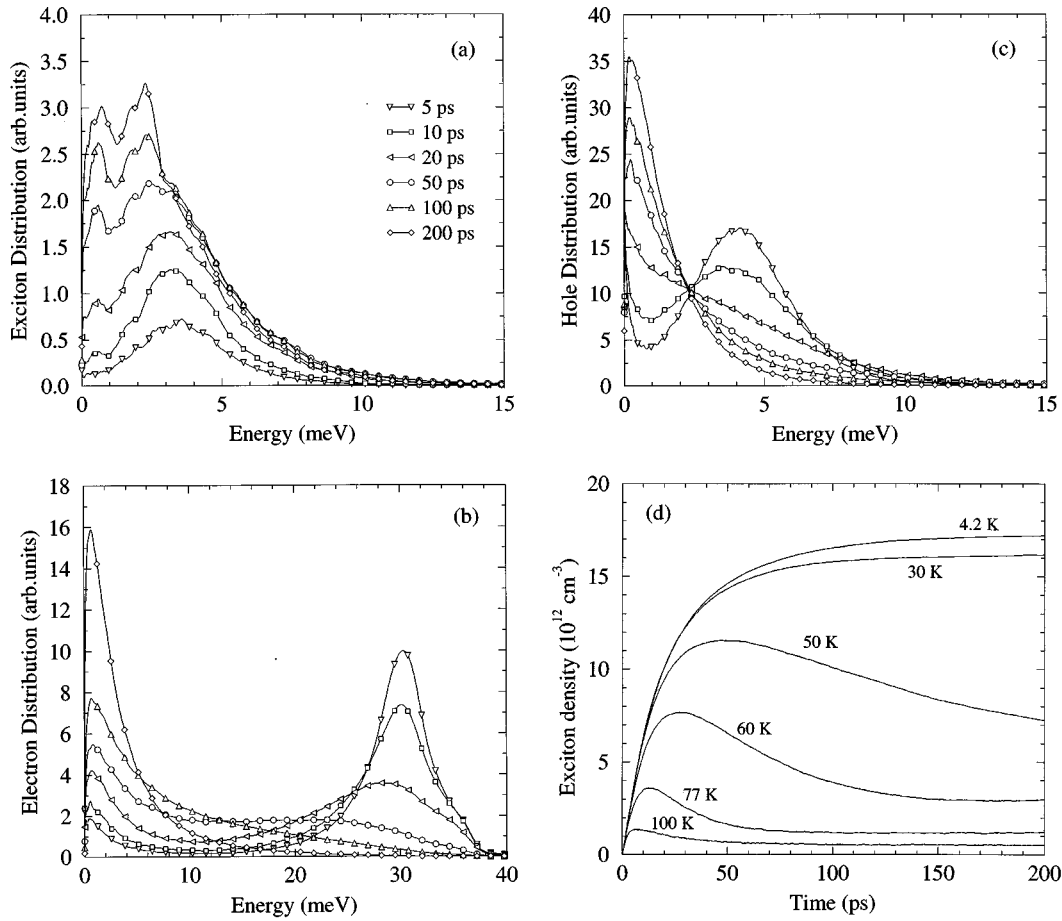


FIG. 5. Relaxation after optical excitation with a Gaussian laser pulse of 500 fs duration and excess energy of $\Delta E = 34$ meV over the gap. The final pair density is 10^{14} cm^{-3} . Distribution functions of electrons (a), holes (b), and excitons (c) at different times. (d) Temporal evolution of the total exciton density for different lattice temperatures.

to broadening. The exciton distribution, shown in Fig. 6(a) on the same scale as in Fig. 5(a), rises much more slowly and is less structured: the hole energies are larger on average and more spread. Exciton states with higher energies are populated compared to the previous case. The effect of the different excitation conditions is perhaps best seen when comparing Figs. 5(d) and 6(d): in the ORE case the total exciton density is lowered by, roughly speaking, a factor of 2 and increases more slowly for all temperatures. Ionization is unimportant for low temperatures, as before. But, for higher temperatures, the formation is no longer much faster and the overshooting behavior of n_X is practically absent.

The comparison of the two simulations demonstrates that the kinetics of the exciton-formation process have a sensitive dependence on the excess energy of the laser pulse, which is explained by inspection of the transition probability for LO-phonon-mediated binding (Fig. 2).

B. Oscillatory dependence on the laser excess energy

The photoconductivity and the photoluminescence of bulk GaAs under steady state excitation are known to exhibit an oscillatory dependence on the optical excitation energy,⁴⁶ which is explained in terms of systematic variations of the electron temperature. If, and under which conditions, similar oscillations can be observed in ultrafast time-resolved ex-

periments of the type considered here are less clear. Damen *et al.*²¹ have found no dependence of their results for GaAs quantum wells on laser energy. Blom *et al.*²⁴ have measured the rise time of excitonic luminescence in thin GaAs quantum wells. They report clear oscillations of this quantity and interpret this result as the occurrence of a selective LO-phonon-assisted exciton formation. It is assumed that the binding of electrons and holes into excitons is sensitive to the positions of the free particles after the initial LO-phonon cascade. The process has a high probability in certain regions of phase space, which they call “sensitive spots.”

This concept is in accordance with our results for the transition probabilities. We have performed a series of simulations with different laser excess energies.⁴⁸ A result is given in Fig. 7, which compares the time dependence of the total exciton density n_X within the first 200 ps after 500 fs pulses of different energies. The values of lattice temperature (4.2 K) and the final pair density (10^{14} cm^{-3}) are kept fixed. The upper three curves correspond to RE, where the initial peak of the electron distribution or its first or second phonon satellite coincide with the sensitive spot. The condition for the lower three curves is ORE. The results for $\Delta E = 34$ and 76 meV are quite similar: a rapid increase of n_X is followed by saturation at values slightly above $1.5 \times 10^{13} \text{ cm}^{-3}$. ORE, in turns, yields in all cases a remarkably slower exciton pro-

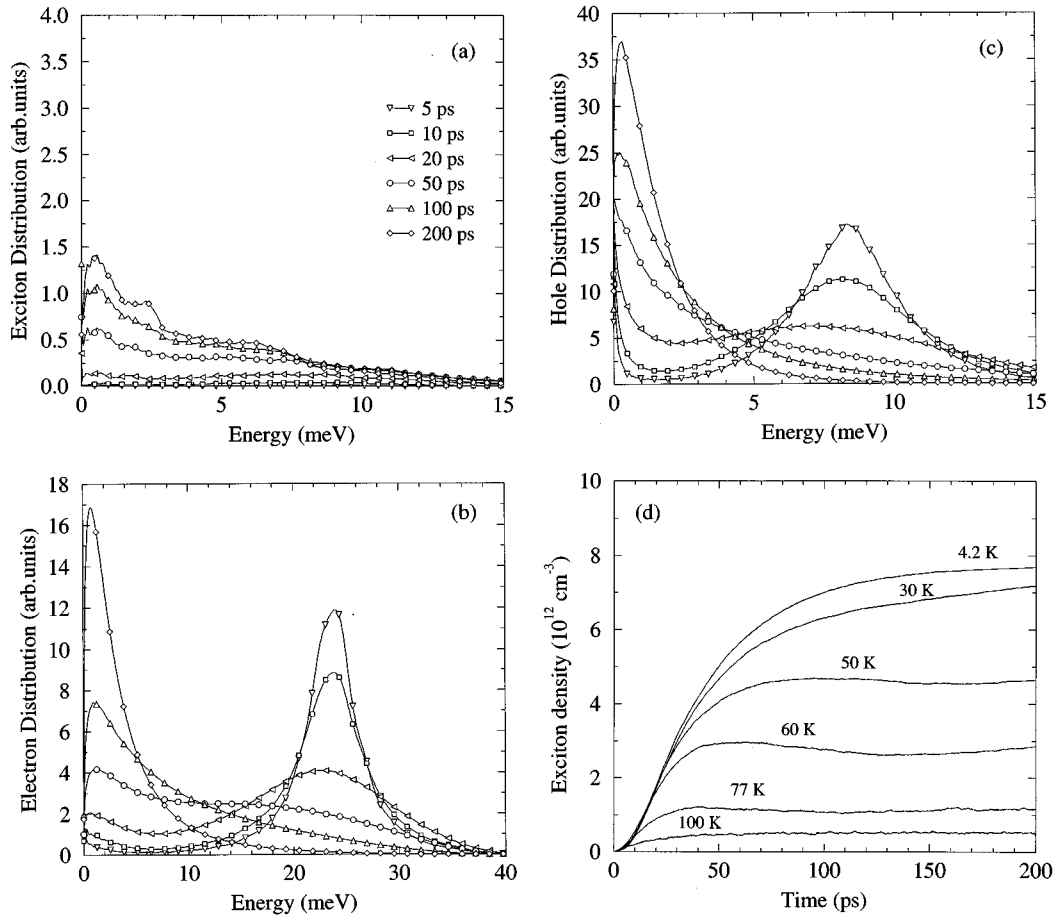


FIG. 6. Relaxation after optical excitation with an excess energy of $\Delta E = 68$ meV over the gap. The other parameters are those of Fig. 5. Distribution functions of electrons (a), holes (b), and excitons (c) at different times. (d) Temporal evolution of the total exciton density for different lattice temperatures.

duction and smaller final values of $n_X \approx 8 \times 10^{12} \text{ cm}^{-3}$. The curve for $\Delta E = 117$ meV is in between, concerning both the slope and the saturation density. During the LO-phonon cascade—it is the second satellite that is on the sensitive spot—the electron distribution has already been broadened to a large extent.

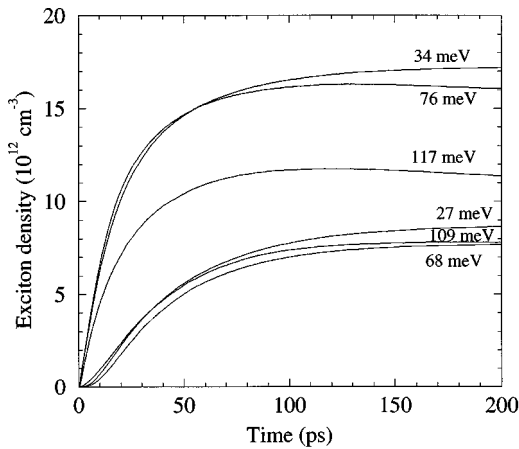


FIG. 7. Time dependence of the total density of excitons for various laser energies. The final pair density is 10^{14} cm^{-3} and the lattice temperature 4.2 K. Labels on the curves give the mean excess energies of the generated e - h pairs.

The density n_X itself is not observed in the experiments. Excitons are created at several meV above the band edge and have to be scattered into states close to $K=0$ before they can recombine radiatively. The measured time dependence of the luminescence signal will reflect the intrinsic formation time *and* the time needed to relax within the exciton band. We have determined the potentially “radiative” fraction of excitons within the homogeneous linewidth,²⁶ Δ , by integration over the distribution function:

$$\delta n_X(t) \propto \int_0^\Delta d\epsilon \rho(\epsilon) f_X(\epsilon) \quad (4.3)$$

[$\rho(\epsilon)$ is the density of states]. It is assumed that the luminescence intensity is proportional to this quantity: $I(t) \propto \delta n_X(t)$. A two-parameter exponential fit of the form

$$I(t) = I_0(1 - e^{-(t-\tau_0)/\tau_R}) \quad (4.4)$$

yields the rise time of luminescence, τ_R . The introduction of a delay time τ_0 substantially improves the fit, especially for ORE. As shown before, the sharp structures in the electron distribution are broadened with increasing time and particles are scattered up in energy, where they can bind. Furthermore, the initial mean energy of the excitons in the 1s band (and its variance) depends on ΔE . τ_0 accounts for just these facts.

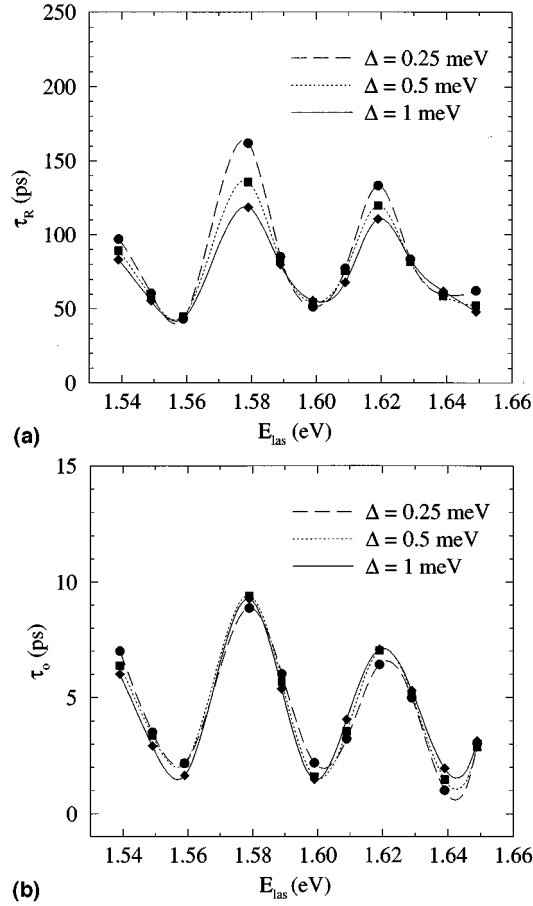


FIG. 8. Rise time of luminescence τ_R (a) and delay time τ_0 (b) as obtained from a two-parameter exponential fit (see text) for three values of the homogeneous linewidth Δ as a function of the laser energy.

Figure 8 presents the results for τ_R and τ_0 which have been obtained assuming three different values for the homogeneous linewidth Δ . For both quantities we find an oscillatory dependence on laser energy with period $\hbar\omega_0(1+m_e/m_h)$ as expected⁴⁶ for a mechanism that relies on LO-phonon-related structures in the electron distribution function. The rise time of luminescence τ_R , Fig. 8(a), has minima of ≈ 50 ps at energies that correspond to RE. The maxima for ORE depend on the value chosen for the linewidth Δ and lie in the range of 100–150 ps. A similar behavior is found for the delay time τ_0 on a much shorter time scale [Fig. 8(b)].

It is not only the time evolution of the generated exciton density that changes in a systematic way with the laser energy, but its maximum value finally reached, too. It has to be expected that the *integrated* luminescence, which is proportional to the time integral of (4.3), will depend on ΔE . This is indeed the case as can be seen in Fig. 9. The (relative) luminescence intensity integrated over the first 200 ps after the pulse has minima at energies where the LO-phonon-related formation process is slow and not very effective (maxima in Fig. 8).

The sharp structures in the transition probability, Fig. 2, are the basis for the results of this subsection. As discussed, they are always present and there are in fact possible “sensitive spots” for phonon-assisted excitonic binding. How-

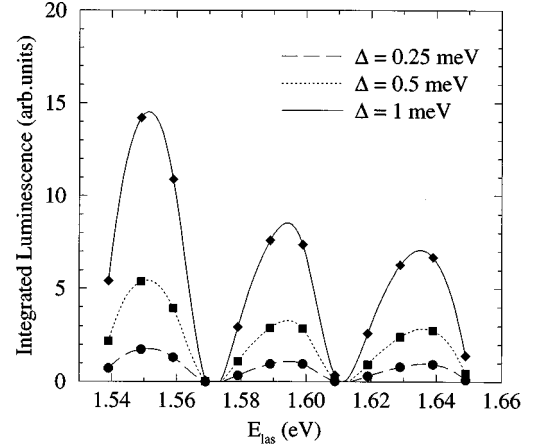


FIG. 9. Calculated time-integrated luminescence signal vs energy of the exciting laser for three values of the homogeneous linewidth Δ .

ever, the other prerequisite, the sharply peaked electron distribution function, is obtained under certain conditions only. The laser pulse must not be too short to avoid the generation of a broad initial distribution due to energy-time uncertainty. Further, in simulations for higher temperatures and densities (where the scattering mechanisms that broaden the electron distribution gain importance) the oscillations found in luminescence are strongly damped. The same has to be expected for a more realistic band-structure model. The inclusion of more than just one (heavy) hole band and of valence-band warping may lead to additional smearing of the structures in f_e and reduce the effects.

As a final application of our theory we will present results for low-temperature simulations of RE with $\Delta E = 34$ meV for different final pair densities n_0 , i.e., for different intensities of the exciting laser pulse. The rate of our exciton-formation mechanism, is of course, density dependent, since it depends on the occupation of the initial free-carrier states. The Coulomb scattering among the free carriers is important for the shape of their distribution functions and influences the physical processes in the system in another, nontrivial way.

Figure 10 reveals that increasing the particle density quickens the initial buildup of the exciton distribution. For comparison we have plotted the total exciton density normalized to the final pair density n_0 . The excitation conditions are again those of Fig. 5: electrons are generated 30 meV above the band edge on the sensitive spot and the lattice temperature is 4.2 K. For the lowest simulated density a steady slow increase of n_X during 200 ps is found. Finally, only a fraction of 8% of e - h pairs are bound into excitons. At higher densities the initial phase of rapid binding shortens and is followed by a much slower increase of the population. The overall efficiency of the exciton formation increases and the final densities n_X at $t = 200$ ps scale with the total density of generated e - h pairs n_0 approximately as $n_X \propto n_0^\gamma$ with an exponent $\gamma = 1.3$. A rate-equation analysis for steady state excitations (where some additional loss mechanism like free-carrier and exciton recombination has to be introduced explicitly to obtain stationary solutions) would give⁴⁶ $n_X \propto n_0^2$. Although both cases cannot be compared directly, it becomes

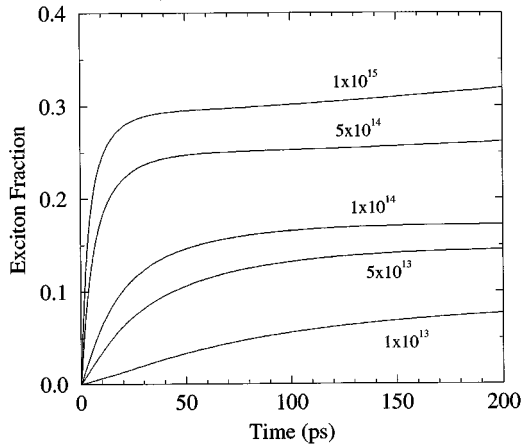


FIG. 10. Time evolution of the fraction of excitons for different final densities of e - h pairs at $T=4.2$ K.

apparent again that the free carriers do not take part in the exciton formation in a common way but according to their time-dependent microscopic distribution functions.

V. SUMMARY AND OUTLOOK

The main purpose of this paper was the development of a consistent semiclassical model of the coupled relaxation kinetics of free carriers and excitons in semiconductors after ultrafast optical excitation at energies high in the bands in the low-density regime. This has been achieved by an extension of the system of free-carrier Boltzmann equations by a similar equation for the distribution function of $1s$ excitons. Transition probabilities have been calculated quantum mechanically for intraband scattering of excitons as well as for phonon-mediated exciton binding and dissociation processes using Fermi's golden rule. For the solution of the resulting system of kinetic equations, an ensemble Monte Carlo method based on a cell discretization in \vec{k} space has been extended to include the exciton distribution and the various reaction mechanisms that transmute free e - h pairs into excitons, and vice versa.

The simulation method has been applied to a simple two-band model of a bulk semiconductor with parameters typical for GaAs. It has been found that the pronounced energy dependence of the probabilities for LO-phonon-assisted transitions between free-pair states and excitons has a strong influence on the efficiency of the exciton formation process and on the temporal evolution of the resulting population. By varying the energy of the exciting laser, it is possible to generate an initial electron distribution such that it peaks in a region in phase space with a high or a low probability for

exciton formation, respectively, after the initial LO-phonon cascade. This has a systematic effect on the rise time of luminescence and on the time-integrated luminescence. Even for the low excitation intensities considered here, the formation kinetics turn out to be strongly density dependent, partly due to the fact that the elementary binding requires the simultaneous presence of an electron and a hole in a given phase-space volume, and partly because the shape of the free-carrier distributions is influenced by carrier-carrier scattering.

For two reasons we see this investigation as the starting point for further work in the field. First, we have considered up to now just the exciton-phonon interaction as responsible for intrinsic formation, dissociation, and relaxation of excitons. These are to lowest order the most important processes in the low-density limit. However, it is desirable to include exciton-exciton scattering, which acts to establish a quasi-equilibrium within the distribution, and exciton-free-carrier interaction. Also, competing mechanisms such as free-carrier capture by impurities⁴⁹ could be considered.

The second reason is even more important. Here we have presented model calculations for a bulk semiconductor. In the case of GaAs it has to be expected that the *absolute* emitted luminescence intensity is rather small and difficult to observe with appropriate time resolution. Nonintrinsic processes like impurity-bound exciton recombination will tend to overwhelm the free-exciton recombination⁵⁰ and thus mask the predicted effects even in high-quality bulk material. The situation becomes much better in quasi-two-dimensional systems like quantum wells: the additional spatial confinement of the exciton enhances its binding energy and oscillator strength¹⁸ and perturbing processes are reduced.⁵⁰ Consequently, intrinsic excitonic effects are better observed and this explains why time resolved experiments of the type considered here have been performed solely on quantum wells. The present kinetic model can be applied to such systems by a proper choice of the free-particle and exciton basis states and the numerical method can be generalized. It will be, however, necessary to include the radiative recombination of excitons as a loss mechanism since it will act in an effective manner at shorter times due to the increased optical matrix element. The application of our approach to quantum wells is under way and will lead us to a direct comparison of theoretical results with experimental data.

ACKNOWLEDGMENTS

P.E.S. wishes to thank R. Zimmermann for many stimulating discussions. This work was supported in part by the European Commission through the HCM network "ULTRAFAST."

¹See, e.g., U. Keller, in *Photons and Local Probes*, edited by O. Marti and R. Möller (Kluwer Academic, Dordrecht, 1995), p. 295, and references therein.

²J. Shah, *Solid-State Electron.* **32**, 1051 (1989).

³H. Kurz, *Semicond. Sci. Technol.* **7**, B124 (1992).

⁴W. Pötz and P. Kocevar, *Phys. Rev. B* **28**, 7040 (1983).

⁵M. Asche and O.G. Sarbei, *Phys. Status Solidi B* **141**, 487 (1987).

⁶T.F. Zheng, W. Cai, P. Hu, and M. Lax, *Solid-State Electron.* **32**, 1089 (1989).

⁷K. Leo and J.H. Collet, *Phys. Rev. B* **44**, 5535 (1991).

⁸A.A. Grinberg and S. Luryi, *Phys. Rev. Lett.* **65**, 1251 (1990); A.A. Grinberg, S. Luryi, N.L. Schryer, R.K. Smith, C. Lee, U.

- Ravaioli, and E. Sangiorgi, Phys. Rev. B **44**, 10 536 (1991).
- ⁹J. Collet and T. Amand, Physica **134B**, 394 (1985).
- ¹⁰R. Binder, D. Scott, A.E. Paul, M. Lindberg, K. Henneberger, and S.W. Koch, Phys. Rev. B **45**, 1107 (1992).
- ¹¹K. El Sayed, T. Wicht, H. Haug, and L. Bányai, Z. Phys. B **86**, 345 (1992).
- ¹²M.A. Osman and D.K. Ferry, Phys. Rev. B **36**, 6018 (1987).
- ¹³P. Lugli, P. Bordone, L. Reggiani, M. Rieger, P. Kocevar, and S.M. Goodnick, Phys. Rev. B **39**, 7852 (1989).
- ¹⁴D.W. Bailey, C.J. Stanton, and K. Hess, Phys. Rev. B **42**, 3423 (1990).
- ¹⁵T. Elsaesser, J. Shah, L. Rota, and P. Lugli, Phys. Rev. Lett. **66**, 1757 (1991).
- ¹⁶T. Kuhn and F. Rossi, Phys. Rev. B **46**, 7496 (1992).
- ¹⁷U. Hohenester, P. Supanic, P. Kocevar, X.Q. Zhou, W. Kütt, and H. Kurz, Phys. Rev. B **47**, 13 233 (1993).
- ¹⁸H. Haug and S.W. Koch, *Quantum Theory of the Optical and Electronic Properties of Semiconductors* (World Scientific, Singapore, 1994).
- ¹⁹T. Amand, B. Dareys, B. Baylac, X. Marie, J. Barrau, M. Brousseau, D.J. Dunstan, and R. Planel, Phys. Rev. B **50**, 11 624 (1994).
- ²⁰J. Kusano, Y. Segawa, Y. Aoyagi, S. Namba, and H. Okamoto, Phys. Rev. B **40**, 1685 (1989).
- ²¹T.C. Damen, J. Shah, D.Y. Oberli, D.S. Chemla, J.E. Cunningham, and J.M. Kuo, Phys. Rev. B **42**, 7434 (1990).
- ²²R. Strobel, R. Eccleston, J. Kuhl, and K. Köhler, Phys. Rev. B **43**, 12 564 (1991).
- ²³Ph. Roussignol, C. Delalande, A. Vinattieri, L. Carraresi, and M. Colocci, Phys. Rev. B **45**, 6965 (1992).
- ²⁴P.W.M. Blom, P.J. van Hall, C. Smit, J.P. Cuypers, and J.H. Wolter, Phys. Rev. Lett. **71**, 3878 (1993).
- ²⁵D. Robart, X. Marie, B. Baylac, T. Amand, M. Brousseau, G. Bacquet, G. Debart, R. Planel, and J.M. Gerard, Solid State Commun. **95**, 287 (1995).
- ²⁶J. Feldmann, G. Peter, E.O. Göbel, P. Dawson, K. Moore, C. Foxon, and R.J. Elliott, Phys. Rev. Lett. **59**, 2337 (1987).
- ²⁷R. Zimmermann, *Many-Particle Theory of Highly Excited Semiconductors* (Teubner Verlagsgesellschaft, Leipzig, 1988).
- ²⁸Yu.L. Klimontovich, Sov. Phys. JETP **25**, 820 (1967); **27**, 75 (1968).
- ²⁹M. Lindberg and S.W. Koch, Phys. Rev. B **38**, 3342 (1988).
- ³⁰S. Haas, F. Rossi, and T. Kuhn, Phys. Rev. B **53**, 12 855 (1996).
- ³¹V.M. Axt and A. Stahl, Z. Phys. B **93**, 195 (1994); **93**, 205 (1994).
- ³²A. Leitenstorfer *et al.*, Phys. Rev. Lett. **73**, 1687 (1994).
- ³³As usual, we neglect possible interband transitions caused by the interactions considered here.
- ³⁴T. Takagahara, Phys. Rev. B **31**, 6552 (1985).
- ³⁵L.D. Landau and E.M. Lifshitz, *Quantum Mechanics—Nonrelativistic Theory* (Pergamon, London, 1965).
- ³⁶S. Permogorov, Phys. Status Solidi B **68**, 9 (1975).
- ³⁷R.J. Elliott, Phys. Rev. **108**, 1384 (1957).
- ³⁸A.I. Anselm and Yu.A. Firsov, Zh. Éksp. Teor. Fiz. **28**, 151 (1955) [Sov. Phys. JETP **1**, 139 (1955)]; Y. Toyozawa, Prog. Theor. Phys. **20**, 53 (1958). For a review, see J. Singh, Solid State Phys. **38**, 295 (1984).
- ³⁹A. Garcia-Cristobal, A. Cantarero, C. Trallero-Giner, and M. Cardona, Phys. Rev. B **49**, 13 430 (1994).
- ⁴⁰S. Rudin, T.L. Reinecke, and B. Segall, Phys. Rev. B **42**, 11 218 (1990); **52**, 11 517 (1995).
- ⁴¹S. Rudin and T.L. Reinecke, Phys. Rev. B **41**, 3017 (1990).
- ⁴²J. Lee, E.S. Koteles, and M.O. Vassel, Phys. Rev. B **33**, 5512 (1986); H.N. Spector, J. Lee, and P. Melman, *ibid.* **34**, 2554 (1986).
- ⁴³C. Jacoboni and L. Reggiani, Rev. Mod. Phys. **55**, 645 (1983).
- ⁴⁴C. Jacoboni and P. Lugli, *The Monte Carlo Method for Semiconductor Device Simulations* (Springer, Vienna, 1989).
- ⁴⁵K. Kometer, G. Zandler, and P. Vogl, Semicond. Sci. Technol. **7**, B559 (1992).
- ⁴⁶C. Weisbuch, Solid-State Electron. **21**, 179 (1978).
- ⁴⁷The temperature dependence of the gap energy has been corrected for, and it is the *excess* energy of the laser that is kept fixed.
- ⁴⁸Preliminary results will appear in P. E. Selbmann, M. Gulia, F. Rossi, E. Molinari, and P. Lugli, in Proceedings of the 9th International Conference on Hot Carriers in Semiconductors, Chicago, 1995, edited by J.-P. Leburton, U. Ravaioli, and K. Hess (Plenum, New York, in press).
- ⁴⁹R. Ulbrich, Phys. Rev. Lett. **27**, 1512 (1971).
- ⁵⁰C.I. Harris *et al.*, Phys. Rev. B **50**, 18 367 (1994), and references therein.